Dark Energy Reflections in the Redshift-Space Quadrupole

Kazuhiro Yamamoto,[1] Bruce A. Bassett,[2,3] and Hiroaki Nishioka[4]

[1]*Department of Physical Science, Hiroshima University, Higashi-Hiroshima, 739-8526, Japan*
[2]*Department of Physics, Kyoto University, Kyoto,739-8502, Japan*
[3]*ICG, University of Portsmouth, PO12EG, England*
[4]*Institute of Astronomy and Astrophysics, Academia Sinica, Taipei 106, Taiwan, Republic of China*

(Received 8 September 2004; published 9 February 2005)

We show that the redshift-space quadrupole will be a powerful tool for constraining dark energy even if the baryon oscillations are missing from the monopole power spectrum and bias is scale and time dependent. We calculate the accuracy with which next-generation galaxy surveys such as KAOS will measure the quadrupole power spectrum, which gives the leading anisotropies in the power spectrum in redshift space due to linear velocity, and the so-called "Finger of God" and Alcock-Paczynski effects. Combining the monopole and quadrupole power spectra, in the complete absence of baryon oscillations ($\Omega_b = 0$), leads to a roughly 500% improvement in constraints on dark energy compared with those from the monopole spectrum alone.

DOI: 10.1103/PhysRevLett.94.051301 PACS numbers: 98.62.Py, 95.35.+d, 98.80.Es

Introduction.—The promise of next-generation galaxy surveys such as the Kilo-Aperture Optical Spectrograph (KAOS [1]) is to map the distribution of about one million galaxies in the redshift range $z = 0.5$–3.5. This redshift coverage will allow the baryon oscillations in the matter power spectrum to be followed as they were stretched by the cosmic expansion, thus providing us with a standard ruler with which to precisely measure the extragalactic distance scale and expansion rate [2–7].

However, this technique relies crucially on the assumption that the baryon oscillations will be detected. Although there are tentative indications for this at low z in the two-degree field (2df) data [8,9] the jury is still out on their existence. If bias turns out to be much more complicated than we think or Ω_b is unexpectedly low, we may face an essentially featureless galaxy power spectrum that is too slippery to supply a standard ruler. In that case it is natural to ask whether surveys such as KAOS will yield any constraints on dark energy at all.

The aim of this Letter is to show that *even* in this worst case scenario, next-generation surveys will be able to deliver good constraints on dark energy through a very different route: redshift-space anisotropies and the Alcock-Paczynski (AP) effect [9–14].

In general the power spectrum *in redshift space* is not isotropic; an effect already seen in the 2df survey [15]. There is a linear distortion due to the bulk motion of the sources within the linear theory of density perturbation [16], while the so-called "finger of God" effect causes radial elongations due to the motion of galaxies in the nonlinear regime [17]. In addition there is a geometric distortion due to the AP effect related to the distance-redshift relation of the Universe. As a result the redshift-space power spectrum depends on the angle θ between the line-of-sight direction γ and the wave number vector $\mathbf{k}$ (see, e.g., [18]).

In general the redshift-space power spectrum can be expanded as [19]

$$P(\mathbf{k}, z) = P(k, \mu, z) = \sum_{l=0,2,4,\cdots} P_l(k, z)\mathcal{L}_l(\mu), \quad (1)$$

where $\mathcal{L}_l(\mu)$ is the Legendre polynomial, $\mu = \cos\theta$, and $k = |\mathbf{k}|$. The odd moments vanish by symmetry.

The monopole $P_0(k, z)$ represents the angular averaged power spectrum and is usually what we mean by the power spectrum. At low z it has been investigated in great depth in the 2df and Sloan Digital Sky Survey surveys. $P_2(k, z)$ is the quadrupole spectrum and gives the leading anisotropic contribution. As can be seen in Fig. 1 it will be well constrained even by just the $z < 1.5$ sample, which we

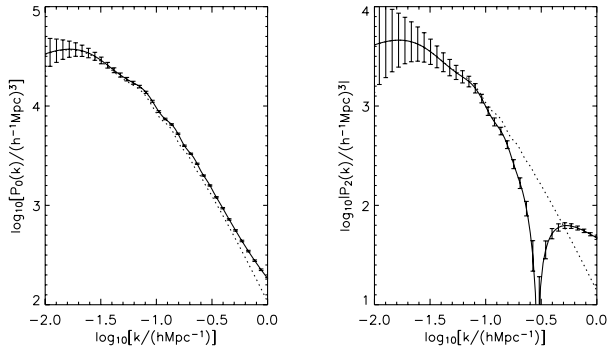

FIG. 1. KAOS1 constraints ($z < 1.5$) on the multipole moments of the power spectrum, $\langle \mathcal{P}_0(k) \rangle$ and $\langle \mathcal{P}_2(k) \rangle$ for linear (dotted lines) and nonlinear (solid lines) spectra, respectively. The nonlinear $\langle \mathcal{P}_2(k) \rangle$ prediction changes sign at large k. We have fixed $n = 1$, $h = 0.7$, $\Omega_b = 0.045$, $\Omega_m = 0.28$, and $w = -1$. For the bias we adopted $b_0 = 1.35$, $p_0 = 1$ for the linear model, $p_1 = 1$, $b_1 = 0.1$, $\nu = 1$ for the nonlinear spectrum [see Eq. (7)]. The higher moments $\mathcal{P}_\ell$, $\ell \geq 4$ are not well constrained, even by KAOS.

label KAOS1 (see Table I for definitions). The higher-order multipoles are not well constrained however.

Crucially, the multipole moments reflect different aspects of the redshift distortions in the power spectrum which can therefore aid in breaking degeneracies between the cosmological parameters bias and dark energy. The purpose of this Letter is to consider the extent to which the anisotropic component of the power spectrum, P_ℓ, $\ell \geq 2$, gives new information about dark energy via the nonlinear effects and the geometric (AP) distortion.

Formalism.—Here we employ the Fisher matrix approach in order to estimate the accuracy with which we can constrain the equation of state, $w \equiv p/\rho$, of the dark energy with a measurement of the power spectrum. In general the Fisher matrix is defined by $F_{ij} = -\langle \partial^2 \ln L/\partial\theta_i \partial\theta_j \rangle$, where L is the likelihood of a data set given the model parameters θ_i. Assuming a Gaussian probability distribution function for the errors of a measurement of the multipole power spectrum $\mathcal{P}_l(k)$, the Fisher matrix for each multipole spectrum is

$$F_{ij}^{(l)} \simeq \frac{1}{4\pi} \int_{k_{\rm min}}^{k_{\rm max}} \kappa_l(k) \frac{\partial \langle \mathcal{P}_l(k) \rangle}{\partial \theta_i} \frac{\partial \langle \mathcal{P}_l(k) \rangle}{\partial \theta_j} k^3 d\ln k, \quad (2)$$

where $\kappa_l(k)$ is the effective volume of the survey available for measuring the ℓth power spectrum at wave number k:

$$\kappa_l(k)^{-1} = \frac{1}{2} \int_{-1}^{1} d\mu \frac{\int d\mathbf{s} \bar{n}(\mathbf{s})^4 \psi(\mathbf{s}, k, \mu)^4 [P(k, \mu, z) + 1/\bar{n}(\mathbf{s})]^2 [\mathcal{L}_l(\mu)]^2}{[\int d\mathbf{s}' \bar{n}(\mathbf{s}')^2 \psi(\mathbf{s}', k, \mu)^2]^2}, \quad (3)$$

and

$$\langle \mathcal{P}_l(k) \rangle = \frac{1}{2} \int_{-1}^{1} d\mu \frac{\int d\mathbf{s} \bar{n}(\mathbf{s})^2 \psi(\mathbf{s}, k, \mu)^2 P(k, \mu, z) \mathcal{L}_l(\mu)}{\int d\mathbf{s}' \bar{n}^2(\mathbf{s}') \psi(\mathbf{s}', k, \mu)^2}, \quad (4)$$

where $\psi(\mathbf{s}, k, \mu)$ is a weight factor that we can choose freely, $\bar{n}(\mathbf{s})$ is the mean number density, and $\mathbf{s}$ denotes the three dimensional coordinate in redshift space. This formula can be derived in a similar way to obtain the optimal weighting scheme (see, e.g., [12,20]). Minimizing the variance on the power spectrum yields $\psi(\mathbf{s}, k, \mu) = [1 + \bar{n}(\mathbf{s}) P(k, \mu, z)]^{-1}$, the same as used in [5].

Next we explain our theoretical modeling of the power spectrum. In a redshift survey, the redshift z is the indicator of the distance. Therefore we need to assume a distance-redshift relation $s = |\mathbf{s}| = s[z]$ to plot a map of objects. The power spectrum depends on this choice of the radial coordinate of the map $s = s[z]$ due to the geometric distortion (AP) effect. For our fiducial background we adopt a flat universe with $\Omega_m = 0.3$. We consider a cosmological model with the dark energy component with constant equation of state, $w \equiv p/\rho$, since estimates for the nonlinear power spectrum in more general cases do not yet exist. We then have

$$r(z, \Omega_m, w) = \frac{1}{H_0} \int_0^z \frac{dz'}{\sqrt{\Omega_m (1 + z')^3 + (1 - \Omega_m)(1 + z')^{-3(1+w)}}}. \quad (5)$$

Here $H_0 = 100h$ km/s/Mpc is the Hubble parameter.

Our fiducial model thus has $s(z) \equiv r(z, 0.3, -1)$. The geometric distortion in the power spectrum depends on $r(z, \Omega_m, w)$ and the power spectrum at redshift z is described by scaling the wave numbers from real space to redshift space via $q_\parallel \to k\mu/c_\parallel$ and $q_\perp \to k\sqrt{1 - \mu^2}/c_\perp$ with $c_\parallel(z) = dr(z)/ds(z)$ and $c_\perp(z) = r(z)/s(z)$.

We write the galaxy power spectrum in nonlinear theory as

$$P_{\rm gal}(q_\parallel, q_\perp, z) = \left(1 + \frac{f(z)}{b(z, q)} \frac{q_\parallel^2}{q^2}\right)^2 b(z, q)^2 P_{\rm mass}^{\rm NL}(q, z) D[q_\parallel \sigma_P(z)], \quad (6)$$

with $f(z) = d\ln D_1(z)/d\ln a(z)$, where $q^2 = q_\parallel^2 + q_\perp^2$, $b(z, q)$ is a scale-dependent bias factor, $P_{\rm mass}^{\rm NL}(q, z)$ is the nonlinear mass power spectrum normalized by $\sigma_8 = 0.9$, $D_1(z)$ is the linear growth rate, and $a(z)$ is the scale factor. The term in proportion to $f(z)$ describes the linear distortion [16]. $D[q_\parallel \sigma_P(z)]$ represents the damping factor due to the "finger of God" effect.

Assuming an exponential distribution function for the pairwise peculiar velocity [21–23] gives $D[q_\parallel \sigma_P(z)] = 1/[1 + (q_\parallel \sigma_P(z))^2/2]$, where $\sigma_P(z)$ is the redshift-dependent one-dimensional pairwise peculiar velocity dispersion as in [21] and Eq. (3.26) in [18]. This form is in excellent agreement with N-body simulations [18].

For $P_{\rm mass}^{\rm NL}(q, z)$ we adopt the fitting formula for the quintessence cosmological model [24] and use the fitting formula for $f(z)$ developed in [25].

For the nonlinear modeling, we assume a scale-dependent bias model with time dependence controlled by $D_1(z)$ (via the parameters b_0, b_1) and three parameters (b_1, p_1, ν) to allow for almost any reasonable scale dependence, viz.

$$b(z, q) = \left(1 + \frac{b_0 - 1}{D_1(z)}\right)\left[1 + b_1 \left(\frac{D_1(z)^{p_1} q}{0.1h \ {\rm Mpc}^{-1}}\right)^\nu\right]. \quad (7)$$

In the linear case the bias is taken to be scale independent and given by $b(z) = 1 + (b_0 - 1) D_1(z)^{-p_0}$ where p_0 is a

constant. The precise form of (7) is not crucial: our aim is to understand the impact of multiple bias parameters on dark energy reconstruction.

Results.—Figure 1 shows the monopole and quadrupole power spectra $\langle \mathcal{P}_0(k) \rangle$ and $\langle \mathcal{P}_2(k) \rangle$ for the linear and nonlinear models described above, assuming the KAOS1 sample described in Table I. $\langle \mathcal{P}_0(k) \rangle$ is positive while the nonlinear effects cause $\langle \mathcal{P}_2(k) \rangle$ to change sign at large k. For $\langle \mathcal{P}_0(k) \rangle$, the linear power spectrum agrees well with the nonlinear power spectrum because the two nonlinear contributions to it cancel out: the "finger of God" effect decreases the amplitude while $P^{\rm NL}_{\rm mass}(k)$ increases the amplitude due to the nonlinearity at large k. By comparison, it is very clear that the linear theory is not good for the higher multipole moments on small scales, $k \gtrsim 0.1h$ Mpc^{-1}.

The precision with which w can be recovered is shown in Fig. 2. We consider separately the low-redshift (KAOS1) and high-redshift (KAOS2) samples; see Table I.

To produce these estimates we quote $\Delta w \equiv (\mathbf{F}^{-1/2})_{ww}$, marginalizing over Ω_m and all the bias parameters, viz. b_0, p_0 (linear case) and b_0, p_1, b_1, and ν (nonlinear case). Since the bias may be constrained by other methods (e.g., lensing or by higher-order correlation functions) our results are conservative.

Figure 2 shows Δw as a function of Ω_b. The left panels are the results for the linear perturbation theory, while the right panels are the nonlinear model. The upper panels assume the KAOS1 sample, while the lower panels assume the KAOS2 sample. In general, Δw becomes larger as the baryon fraction becomes smaller since the baryon oscillations become less and less distinct. As Ω_b becomes smaller, the contribution from $\mathcal{P}_2$ becomes increasingly important. It is clear from the dashed curve that the constraint on w from $\mathcal{P}_0$ is very weak around $\Omega_b = 0$ because the baryon oscillations disappear, taking with it the standard ruler. This is the same for the dotted curve which shows the constraints from $\mathcal{P}_2$.

One of the main results of this paper is the solid curve which shows the constraint from the combination of $\mathcal{P}_0$ and $\mathcal{P}_2$. It is good even in the case $\Omega_b = 0$ when the baryon oscillations are missing, implying that the geometric distortion (AP test) plays the central role in constraining w. This does not depend on the bias parameters and inclusion of a constant parameter for stochastic bias does not alter our results [26].

TABLE I. The parameters of the samples used in our analysis. $\bar{n}$ is the average galaxy number density; $k_{\rm max}$ is the maximum wave number used in evaluating the Fisher matrix.

	KAOS1	KAOS2
Redshift range	$0.5 < z < 1.5$	$2.5 < z < 3.5$
Survey area (deg^2)	10^3	150
$\bar{n}(h^3$ Mpc$^{-3})$	10^{-4}	10^{-4}
$k_{\rm max}(h$ Mpc$^{-1})$	0.4	1
b_0	1.35	1.75

It is interesting to address why the constraint on w from $\mathcal{P}_0$ and $\mathcal{P}_2$ combined is so much better than from either one separately. For each pair of marginalized parameters the error ellipses for $\mathcal{P}_0$ and $\mathcal{P}_2$ are rotated with respect to each other, as in Fig. 3, thus breaking degeneracies in the bias-dark energy parameter space. On marginalization these gains are passed through to w, resulting in significantly smaller error ellipses, a feature observed in both the linear and nonlinear cases. This comes from the fact that the error ellipses for $\mathcal{P}_0$ and $\mathcal{P}_2$ only overlap by a small amount in the full parameter space. The power in combining $\mathcal{P}_0$ and $\mathcal{P}_2$ thus extends the well-known fact that $\mathcal{P}_2$ gives useful information about bias (e.g., [19]).

Conclusions.—We have investigated the accuracy with which we can expect next-generation galaxy surveys such as KAOS [1] to measure the multipole moments of the anisotropic power spectrum in redshift space and the resulting improvements in dark energy constraints.

We found a number of key results: (1) the quadrupole is very useful in breaking degeneracies between bias and dark energy. (2) Nonlinear effects have a substantial influence on the quadrupole and higher multipoles at the scale $k \gtrsim 0.1h$ Mpc^{-1}. The inclusion of the nonlinear power spectrum enhances the precision with which the dark energy can be constrained because the nonlinear effects increase the power at small scale which is also where constraints are good. The nonlinear regime provides us with new infor-

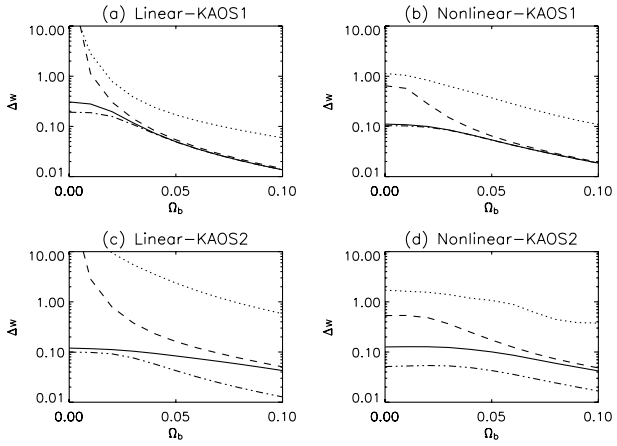

FIG. 2. $1-\sigma$ error estimates for w as the baryon oscillations disappear ($\Omega_b \to 0$). The left panels (a) and (c) are the results using the linear spectrum and the right panels (b) and (d) are the nonlinear spectrum. The dashed curves are the results utilizing *only* $\mathcal{P}_0(k)$, the dotted curves are the results with *only* $\mathcal{P}_2(k)$, the solid curves are the results obtained using *both* $\mathcal{P}_0(k)$ and $\mathcal{P}_2(k)$. The target parameters here are same as those in Fig. 1. The low-redshift sample, KAOS1, is assumed in (a) and (b); the high-redshift sample, KAOS2, is assumed in (c) and (d). The dot-dashed curves in (a) and (b) show the constraints combining all $\mathcal{P}_0(k)$ to $\mathcal{P}_6(k)$. The double dot-dashed curves in (c) and (d) show the constraints obtained from the full KAOS sample (KAOS1 + KAOS2). The key point is how flat the resulting curve is for $\Omega_b \leq 0.05$ despite the absence of baryon oscillations for $\Omega_b \to 0$.

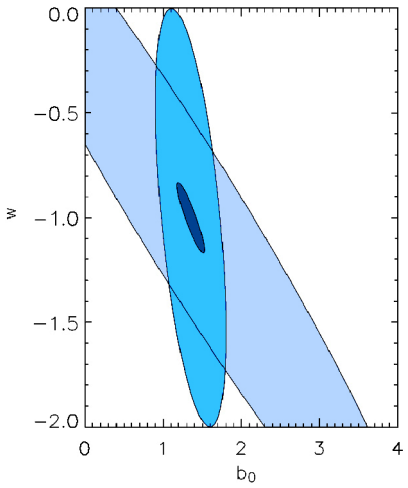

FIG. 3 (color online). $1-\sigma$ $w-b_0$ likelihood contours for $\mathcal{P}_0$ alone (large, vertical ellipse), $\mathcal{P}_2$ alone (largest, lightly-shaded ellipse), and $\mathcal{P}_0+\mathcal{P}_2$ (small, dark ellipse). Here the same parameters are used as in Fig. 1 except that $\Omega_b=0$ so there are no baryon oscillations, which explains the poor constraints from $\mathcal{P}_0$ alone.

mation about the dark energy, as has been discussed in different contexts (e.g., [27]). (3) Applying these results to dark energy and the KAOS survey we have found that significant constraints arise by combining the monopole and quadrupole spectra even if there are no baryon oscillations in the monopole spectrum and even if we allow for multiparameter scale-dependent or stochastic bias.

This is a key piece of insurance for large galaxy surveys given current uncertainty about the existence of baryon oscillations and ensures that large, next-generation, galaxy surveys will make a significant contribution to the hunt for dark energy irrespective of the existence of baryon oscillations.

We thank Daniel Eisenstein and Bob Nichol for comments. This work is supported by a Grant-in-Aid for Scientific Research of the Japanese Ministry of Education, Culture, Sports, Science, and Technology 15740155 and by the Royal Society/JSPS.

[1] A. Dey and B. Boyle, The KAOS Purple Book, http://www.noao.edu/kaos/.
[2] D. Eisenstein, astro-ph/0301623.
[3] C. Blake and K. Glazebrook, Astrophys. J. **594**, 665 (2003).
[4] E. V. Linder, Phys. Rev. D **68** 083504 (2003).
[5] H.-J. Seo and D. J. Eisenstein, Astrophys. J. **598**, 720 (2003).
[6] W. Hu and Z. Haiman, Phys. Rev. D **68** 063004 (2003).
[7] L. Amendola, C. Quercellini, and E. Giallongo, astro-ph/0404599.
[8] C. J. Miller, R. C. Nichol, and X. Chen, Astrophys. J. **579**, 483 (2002).
[9] K. Yamamoto, Astrophys. J. **605**, 620 (2004).
[10] C. Alcock and B. Paczynski, Nature (London) **281**, 358 (1979).
[11] T. Matsubara and A. S. Szalay, Phys. Rev. Lett. **90**, 021302 (2003).
[12] K. Yamamoto, Astrophys. J. **595**, 577 (2003).
[13] W. E. Ballinger, J. A. Peacock, and A. F. Heavens, Mon. Not. R. Astron. Soc. **282**, 877 (1996).
[14] T. Matsubara and Y. Suto, Astrophys. J. **470**, L1 (1996).
[15] J. A. Peacock, *et al.*, Nature (London) **410**, 169 (2001).
[16] N. Kaiser, Mon. Not. R. Astron. Soc. **227**, 1 (1987).
[17] J. A. Peacock and S. J. Dodds, Mon. Not. R. Astron. Soc. **267**, 1020 (1994).
[18] Y. Suto, H. Magira, Y. P. Jing, T. Matsubara, and K. Yamamoto, Prog. Theor. Phys. Suppl. **133**, 183 (1999).
[19] A. N. Taylor and A. J. S. Hamilton, Mon. Not. R. Astron. Soc. **282**, 767 (1996).
[20] H. A. Feldman, N. Kaiser, and J. A. Peacock, Astrophys. J. **426**, 23 (1994).
[21] H-J. Mo, Y. P. Jing, and G. Boerner, Mon. Not. R. Astron. Soc. **286**, 979 (1997).
[22] Y. Suto, H. Magira, and K. Yamamoto, Publ. Astron. Soc. Jpn. **52**, 249 (2000).
[23] H. Magira, Y. P. Jing, and Y. Suto, Astrophys. J. **528**, 30 (2000).
[24] C-P. Ma, R. R. Caldwell, P. Bode, and L. Wang, Astrophys. J. Lett. **521**, L1 (1999).
[25] L. Wang and P. J. Steinhardt, Astrophys. J. **508**, 483 (1998).
[26] M. Tegmark and P. J. E. Peebles, Astrophys. J. **500**, L79 (1998).
[27] J. A. Newman and M. Davis, Astrophys. J. **534**, L11 (2000).